HYDROLOGICAL PROCESSES
Hydrol. Process. (2011)
Published online in Wiley Online Library
(wileyonlinelibrary.com) DOI: 10.1002/hyp.8049

High-resolution monitoring reveals dissolved oxygen dynamics in an Antarctic cryoconite hole

E. A. Bagshaw,[1]* M. Tranter,[1] J. L. Wadham,[1] A. G. Fountain,[2] and M. Mowlem[3]

[1] *Bristol Glaciology Centre, School of Geographical Sciences, University of Bristol, Bristol BS8 1SS UK*
[2] *Departments of Geology and Geography, Portland State University, PO Box 751, Portland, OR 97207-0751 USA*
[3] *National Oceanography Centre, University of Southampton, Waterfront Campus, European Way, Southampton SO14 3ZH UK*

Abstract:

This study presents the first high-resolution dataset of dissolved oxygen (DO) measurements in an ice-lidded cryoconite hole on Canada Glacier, McMurdo Dry Valleys, Antarctica. Fibre optic DO minisensors were installed in a cryoconite hole prior to seasonal internal melting and hydrological connection to the subsurface drainage system. Oxygen air saturation in the cryoconite hole typically ranged from 50 to 80%, in broad agreement with previous single measurements, indicating net respiration (R). This is consistent with results of simple incubation experiments performed in the field. Simultaneous time series for electrical conductivity, water temperature, and DO over the four-week study period provide information regarding the connectivity of cryoconite holes with the near-surface drainage system. The main driver of the observed variations in DO is likely to be periodic melt-freeze cycles. We conclude that automated sensing techniques, such as those described here, when used in conjunction with physical measurements, have great potential for high-resolution monitoring of the factors that perturb biogeochemical processes in cryospheric surface aquatic ecosystems. Copyright © 2011 John Wiley & Sons, Ltd.

KEY WORDS cryoconite hole; oxygen; Antarctica; low temperature biogeochemistry

Received 5 August 2010; Accepted 28 January 2011

INTRODUCTION

Polar ecosystems are sensitive to climate change because small temperature perturbations have large impacts on hydrological and biological processes, via changes in rates of ice and snow melt (Kennedy 1993; Fountain *et al*., 1999; Doran *et al*., 2002; Foreman *et al*., 2004; Esposito *et al*., 2006; Wall 2007). Glacial aquatic environments in the McMurdo Dry Valleys, Antarctica, are model ecosystems for assessing the impacts of climate warming on polar desert environments. Mean summer air temperatures are close to the 0 °C isotherm and the low, spatially limited surface melting (Fountain *et al*., 1999; Hoffman *et al*., 2008) is representative of large sectors of the Earth's cryosphere (e.g. ice sheet interiors) which could potentially 'switch on' and produce meltwater during climate warming.

Limited quantities of glacial meltwater are produced both on the surface and at shallow depths within the ice of these polar glaciers via the solar heating of aerially deposited debris. Meltwater largely flows within, or confined by discrete, ice-topped channels, cryoconite holes (10^{-1} to 5 m in diameter) and larger-scale 'cryo-lakes' ($\sim 10^{1}$ m) (Bagshaw *et al*., 2010a; Tranter *et al*., 2010). The holes and lakes are often linked via a series of surface and subsurface channels (Fountain *et al*., 2004). They are important biogeochemical reactors on the surface of polar glaciers (Tranter *et al*., 2004; Hodson *et al*., 2008; Tranter *et al*., 2010) and provide refugia for life in this extreme polar environment, concentrating biological activity into specific zones on and within the ice surface (Stibal *et al*., 2006; Foreman *et al*., 2007). Cryoconite holes form when debris deposited on the ice surface absorbs solar radiation and melts down into the ice, creating a small, water filled depression (Figure 1). Unlike those in Arctic and temperate regions (Hodson *et al*., 2008), cryoconite holes in the McMurdo Dry Valleys are unique in retaining an ice lid throughout the ablation season (Fountain *et al*., 2004). As a result, cryoconite holes harbour active micro-organisms in self-contained mesocosms which can remain isolated from the hydrological drainage system and the atmosphere for years at a time (Porazinska *et al*., 2004; Tranter *et al*., 2004).

Most information about the biogeochemistry of Antarctic cryoconite holes comes from Canada Glacier, a cold-based glacier in the McMurdo Dry Valleys of Antarctica, where the holes occupy ~4·5% of the ice surface and contain liquid water even when air temperatures are below 0 °C (Fountain *et al*., 2004). About half these holes supply water and solute to downstream cryo-lakes via subsurface channels, while the other half remain hydrologically isolated (Tranter *et al*., 2010). Cryo-lakes form part of a series of frozen-topped pool and riffle systems which can modify the phase and concentrations of solutes supplied by ice melt and cryoconite holes. They are a collection zone for meltwaters before they discharge to the proglacial zone via surface and sub-surface streams

* Correspondence to: E. A. Bagshaw, Bristol Glaciology Centre, School of Geographical Sciences, University of Bristol, Bristol, BS8 1SS UK. E-mail: Liz.Bagshaw@bristol.ac.uk

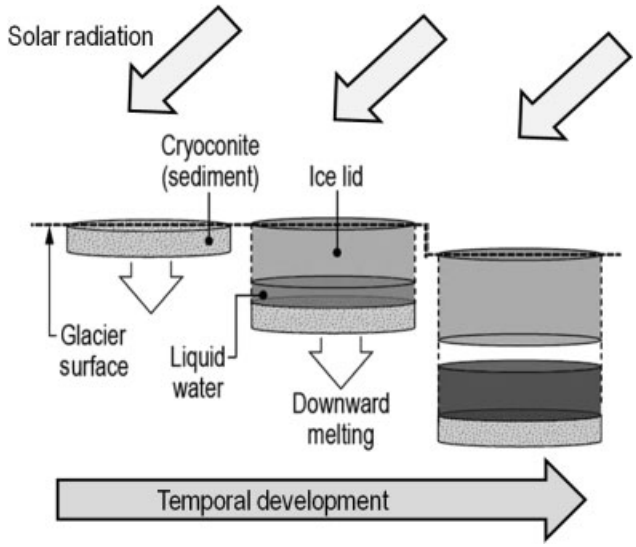

Figure 1. Formation and structure of an Antarctic cryoconite hole (after Cowan and Tow (2004))

(Fountain *et al*., 2004; Fortner *et al*., 2005). Both these environments remain ice covered for much of the melt season, apart from during short, discrete, climate warming events when rapid surface melting, which includes the ice lids of cryoconite holes, triggers a transition to 'open' system conditions. Meltwater volumes, fluxes, and hydrological connectivity increase during this transition (Fortner *et al*., 2005; Doran *et al*., 2008). Manual sampling has shown that organic carbon may be generated in cryoconite holes over time as autotrophic micro-organisms fix carbon dioxide (Bagshaw *et al*., 2007). However, capturing the spatial and temporal variability of these unique and sensitive ecosystems using traditional sampling techniques which are generally destructive, is challenging and may impact on the biogeochemical characteristics of the ecosystem (Bagshaw *et al*., 2010b). For example, Winkler titration requires relatively large sample volumes which cannot then be reused for additional analyses, and Clark-type electrodes require constant stirring, which may disrupt delicate algal films or disturb water column stratification.

The dissolved oxygen (DO) concentration is a key parameter in the estimation of net biological activity in aquatic environments, reflecting the balance between primary production and respiration. Measurement of DO helps determine whether the system is heterotrophic (net C consumption) or autotrophic (net C production) (Anesio *et al*., 2009), and there is currently debate as to whether cryoconite holes are net autotrophic (Sawstrom *et al*., 2002; Anesio *et al*., 2009) or net heterotrophic systems (Stibal *et al*., 2008), and whether the supraglacial drainage system that they form is a net producer or consumer of C as a whole. The use of traditional methods for the determination of DO, such as Winkler titration and Clark-type electrodes, is challenging in the Antarctic environment. Winkler titration requires laboratory equipment, relatively large sample volumes, and usually requires storage of liquid samples fixed with iodine before analysis can occur (Carpenter, 1965). The procedure can be performed with a relatively high level of accuracy in controlled laboratory conditions (Bryan *et al*., 1976), but the challenges of the polar environment may compromise accuracy in the field. The use of Clark-type electrodes is more convenient, but requires relatively large sample volumes and constant stirring (Clark *et al*., 1953). The large probe is generally unsuitable for the small volumes of water generated in the very early melt season. High volumes of sediment, frequently found in the glacial environment, can also interfere with readings.

Consequently, neither Clark-type electrodes nor Winkler titration are suitable methods for determining oxygen concentration continuously over a summer melt season in Arctic or Antarctic micro-niches, such as cryoconite holes (Bagshaw *et al*., 2010b). Most research to date has relied on discrete manual sampling schemes (Tranter *et al*., 2004; Hodson *et al*., 2008; Anesio *et al*., 2009). However, manual sampling is liable to omit key events in the melt season, such as meltwater pulses and freeze-up events. Early and late season processes, in particular, are difficult to sample, yet these events are key to our understanding of how microbial processes switch on and off over the short summer, and how the microbial communities survive the long, dark, winter (Morgan-Kiss *et al*., 2006). Only one study has continuously monitored temperature and electrical conductivity in a series of cryoconite holes, on Canada Glacier over the Austral summers of 2003–2004 and 2005–2006 (Fountain *et al*., 2008). Short periods of rapid and fluctuating change were found, particularly during freeze-thaw cycles at the beginning of the season. The experiment provided excellent detail on the physical and basic chemical processes occurring over the course of the ablation season, but there was little insight into the onset and development of biological activity. We therefore seek new methods for monitoring additional bio-sensitive analytes, such as DO, in supraglacial ecosystems which can operate unattended for prolonged periods.

Fibre optic minisensors were developed in the late 1980s (Lippitsch *et al*., 1988) and early 1990s (Klimant *et al*., 1995) and are now commercially available (Wolfbeis, 2008). They consist of an optical fibre attached to a light source and signal processing unit. The exposed end of the fibre is coated with an immobilized indicator compound which is luminescent and sensitive to the measured parameter (Rogers and Poziomek, 1996). A ruthenium complex is commonly used to measure oxygen. The fibre is illuminated by a light source and the excitation of the luminescent dye molecules is quenched by collision with molecular oxygen. The degree of quenching is proportional to the concentration of oxygen in solution. Fibre optic sensors are advantageous for use in environmental monitoring because they are relatively portable, can measure DO in both gas and liquid phase, do not consume oxygen and do not require stirring. The sensors are sensitive to most organic solvents, but can be used in methanol or ethanol mixtures. They have no cross-sensitivity with CO_2, SO_4^{2-}, Cl^-, NH_4^+ or pH, but interferences may

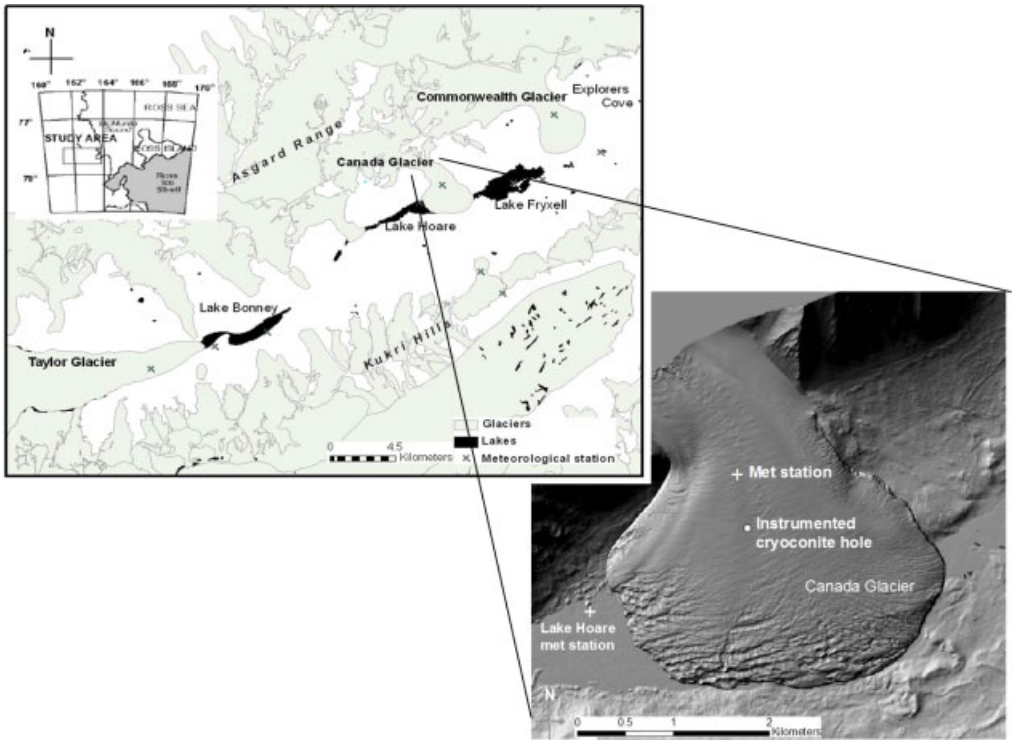

Figure 2. Location of sampling site and meteorological stations on Canada Glacier, Taylor Valley, Antarctica. The inset image is a shaded LiDAR DEM (Light Detection and Ranging Digital Elevation Model)

occur with SO_2 or gaseous Cl_2 (PreSens, 2006). Neither of these interferants is likely to be encountered in significant concentrations in dilute glacial meltwaters.

This paper demonstrates the effectiveness of such optical sensors for the monitoring of DO concentrations in cryoconite holes on Canada Glacier and to reveal for the first time some of the dynamics which determine DO concentrations in these unique ecosystems. Fibre optic minisensors were installed along with conductivity (EC) and temperature (T) probes in a cryoconite hole on the surface of Canada Glacier for four weeks in the Austral summer of 2008–2009. We report the results of this short deployment.

METHODS

Field site

Canada Glacier is located in Taylor Valley (Figure 2), one of the coldest and driest places on Earth, with mean annual temperatures of $-18\,^{\circ}C$ and less than 10 cm (water equivalent) of annual precipitation (Fountain *et al*., 1999; Doran *et al*., 2002). Summer melting on the glacier surfaces is limited, and is often linked to subsurface sediment conglomerations that greatly enhance absorption of solar radiation. The solar heating of the sediment layer within cryoconite holes means that liquid water may be present, sealed beneath an ice cover of 3–20 cm, even when air temperatures are below zero. Enhanced surface melting also occurs on the ice cliffs which flank ice-topped channels and cryolakes as a result of the high angle of incidence of sunlight at the poles (Lewis *et al*., 1999).

The cryoconite hole chosen was 40 cm in diameter and was surrounded by a network of other holes, connected via cracks and old crevasse traces in the ice (Figure 3). This particular hole was chosen since it was highly likely that it would become hydrologically connected to the subsurface drainage system during the thaw, and that the thermal inertia that such a connected hydrological network would provide would maximixe the likelihood of obtaining a continuous time series of DO data. A single cryoconite hole was chosen for monitoring, which was deemed to be representative of a 'typical' hydrologically connected cryoconite hole. The hole was frozen when the DO minisensor and other probes were installed, and melted internally as the ablation season progressed (Fountain *et al*., 2008). The ice lid was intact throughout most of the monitoring period, but it did begin to decay because of melt around the sensor wires and to allow very limited contact with the atmosphere from Day of Year (DY) 345.

The DO minisensor, EC and T probes were introduced to the hole on DY 327 via a 1 cm diameter hole drilled into the ice lid and through the cryoconite hole until just above the sediment layer, and were held in position by a metal spoke (Figure 3). The DO minisensor was installed at a depth of ∼15 cm, some 5 cm above the sediment layer. A second T probe (T2) was installed 10 cm above the DO sensor. Deionized water was poured into the opening of the ice lid and allowed to freeze, so fixing the metal spoke and probes in the hole. It was inevitable that some oxygen was introduced to the hole during the probe insertion, but by fixing the probes into the hole before the seasonal thaw had begun we aimed

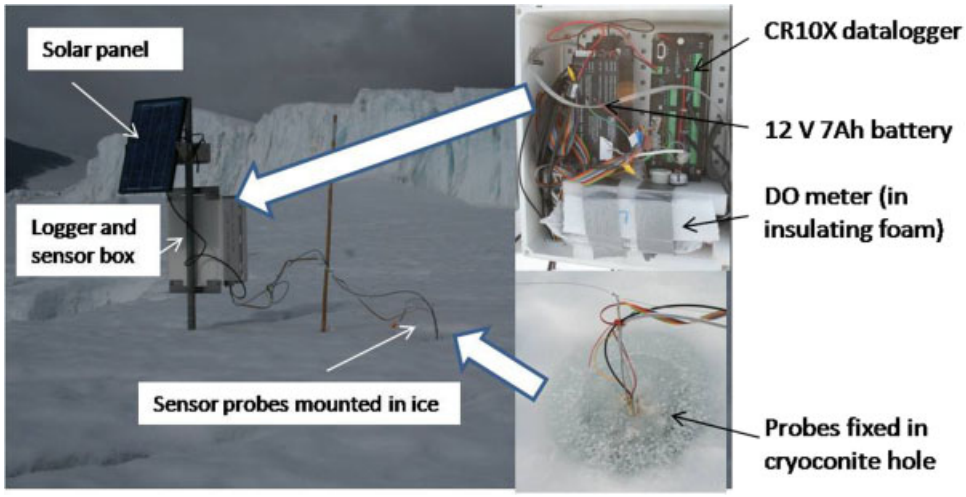

Figure 3. Oxygen sensors installed in a hydrologically connected, ice-lidded cryoconite hole connected on the surface of Canada Glacier. Each sensor is powered by a 7 Ah battery and controlled by a CR10X datalogger

Table I. Mean solute concentration in cryoconite holes on Canada Glacier. Concentrations are in μeq l^{-1}, with the exception of DOC, DIN and DON which are in mg l^{-1}

	Cl^-	NO_3^-	SO_4^{2-}	Na^+	K^+	Mg^{2+}	Ca^{2+}	HCO_3^-	DOC	NH_4^+	NO_3^-	NO_2^-	DIN	DON	PO_4^{3-}	SiO_2
Mean	91·9	6·45	51·1	56·5	15·9	49·8	231	202	0·72	0·97	4·33	0·35	0·07	0·20	—	10·6
St. dev.	93·2	23·3	63·1	46·9	9·02	41·1	145	102	0·32	1·39	5·22	0·47	0·08	0·20	—	7·23
N	89	89	89	89	89	89	89	89	87	73	81	85	89	77	18	89

to mitigate the impacts of this additional oxygen on the overall readings once the hole began to melt. The sensors remained at fixed depth whilst the hole melted into the glacier surface. Water samples were not collected from the hole itself to minimize disturbance, but Table I shows mean solute concentrations from 89 holes sampled on Canada Glacier between 2005 and 2009.

DO minisensor

The DO minisensor used was a Fibox 3 Dipping Probe, manufactured by PreSens (Regensburg, Germany, www.presens.de). It consisted of a 2 mm optical fibre enclosed in a 4 mm diameter, 10 cm long stainless steel tube, connected to an optoelectronic unit for sensor interrogation. The sensing film was immobilized on the fibre tip, and the probe immersed in the cryoconite hole. The fibre was illuminated with an internal LED light source which excited the luminescent dye in the sensing film at the tip of the sensor probes. The phase angle shift between the exciting and emitted light signals is a function of the oxygen partial pressure, and the relative air saturation of oxygen in solution is dependent on temperature and salinity. No salinity correction was required given the generally low EC values measured in our hole (explained below). The oxygen saturation recorded by the datalogger was corrected for temperature, as recorded by the thermistor secured immediately next to the oxygen probe in the cryoconite hole, using a derivative of the Stern-Volmer equation. The saturation changed by no more than 5% as a result of this correction.

The thermistors used were Fenwal Uni-curve type NTC thermistors with a resistance of 2252 Ohms at 25 °C, set in a resin filled vial, and were connected to the datalogger in a 3-wire half bridge configuration using a precision fixed resistor of 255 k Ohms, with low temperature dependence. The thermistors were calibrated in the laboratory across the temperature range −6 to +9 °C. Typical errors quoted for such a thermistor setup and configuration are of the order ±0·03 °C (Ødegärd *et al*., 1997), and arise because of drift over time, calibration slope errors and errors introduced by the datalogger. The EC probe was manufactured from a stainless steel wire set in a resin-filled tube with a separation gap of 5 mm, and calibrated in standard solutions of KCl (full details can be found in Fountain *et al*. (2008)). The EC probe was installed at the same depth as the DO sensor and thermistor. The minisensor and probes were interrogated by a Campbell Scientific CR10X datalogger (Figure 3). Readings were taken every 30 s and an average recorded every 15 min.

Meteorological data were collected on the same timescale at a site on the glacier ∼1·5 km away. Full details of the instrumentation can be found at www.mcmlter.org.

P:R incubations

Incubation experiments were performed in order to measure rates of primary production (P) and respiration (R), and so to derive estimates of the P : R ratio. These data give additional insight into the DO concentrations measured by the automated minisensor by allowing daily

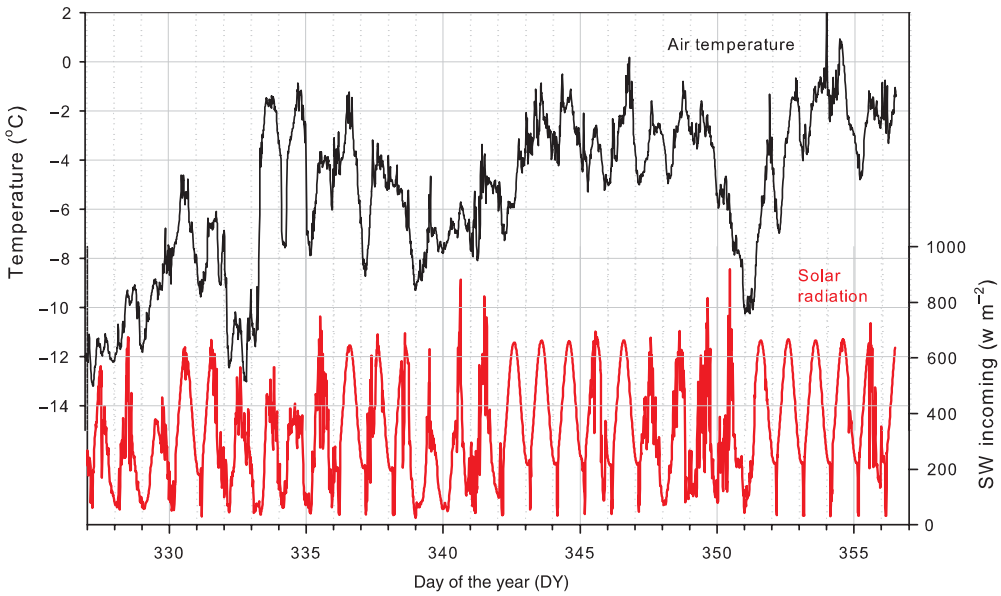

Figure 4. Incoming shortwave solar radiation and air temperature on the glacier surface for the monitoring period in November–December 2008

measurements in strictly controlled environmental conditions. Sediment was collected from the cryolake near to the monitored cryoconite hole, which has a similar debris source to the cryoconite holes. The sediment was incubated in clear glass BOD bottles with glacial melt water collected from a nearby supraglacial stream. Two experiments were run in turn, each with a rock : water ratio of 1 : 2 and a sediment depth of 2 cm, which was the mean found in cryoconite holes on Canada Glacier. In the first, the light, dark, and control bottles were incubated on the lake shore of DLH pond at Lake Hoare camp under ambient environmental conditions. In the second, the bottles were immersed in 10 cm of lake water in order to mimic the light diffusion and relatively constant temperatures found at the bottom of a cryoconite hole. In both experiments, ambient light conditions were similar to those encountered on the surface of Canada Glacier, although there was some additional shading from the glacier sidewalls. Sediment was weighed into each of six bottles and meltwater was poured on top until there was no head space remaining. Three 'dark' bottles were wrapped in aluminium foil to exclude light and so to obtain an estimate of R, while the remaining three bottles were incubated in the light to obtain an estimate of net photosynthesis (P-R). Three blank controls were also incubated, with bottles containing unfiltered supraglacial meltwater only. Bottles were incubated for ~24 h. The water was subsequently carefully decanted and the oxygen saturation measured immediately with a Clark-type YSI 550A oxygen electrode. Fresh meltwater was then added to the sediment and allowed to incubate for a further 24 h. Care was taken to avoid disturbing cyanobacterial films that developed on the surface of the incubated sediment. This procedure was repeated for between 5 and 6 days in total. The temperature of the water remained close to zero during incubation.

P and R as µg C/g/day were calculated by Equations (1) and (2) (Telling *et al.*, 2010), where $O_2{}^{P}$ is the recorded saturation of oxygen in the light sample (%), $O_2{}^{R}$ is the recorded saturation of oxygen in the dark sample (%), $O_2{}^{Blk}$ is the oxygen saturation of the blank, $O_2{}^{0\,^{\circ}C}$ is the oxygen content of water at 0 °C (14 mg/l), 32 is the molecular weight of oxygen, 12 is the atomic weight of carbon and *Hours* is the duration of each incubation step in hours. The equations assume a quotient of unity.

$$P = \frac{(O_2^P - O_2^R)O_2^{0\,^{\circ}C} \cdot Mass_{water} \cdot 12}{32 \cdot Mass_{sediment} \cdot 100 \cdot \left(\frac{Hours}{24}\right)} \quad (1)$$

$$R = \frac{(O_2^{Blk} - O_2^R)O_2^{^{\circ}C} \cdot Mass_{water} \cdot 12}{32 \cdot Mass_{sediment} \cdot 100 \cdot \left(\frac{Hours}{24}\right)} \quad (2)$$

RESULTS

Figure 4 shows the incoming solar radiation (SR) measured at the met station on the glacier from DY 323 to 356. Clear diurnal variations in SR are evident; the sharp decrease for ~1 h at the end of each daily cycle was due to shading from a local peak in the glacier sidewalls. Cloudless days were coincident with smooth variations (for example, DY 343) and cloudy days gave rise to diurnal variations that are relatively spiky. The spiky irradiance maximum on several of the cloudy days appears to exceed the maxima on sunny days; this is an artefact of the instrument mounting. The daily SR peaks became broader as the longest day (DY 355) approached, and hence the net daily SR input to the glacier surface also increased. Figure 4 also shows the air temperatures recorded on the glacier during the same period. Air temperatures oscillated from −13 to −4 °C at the start of the monitoring period, and increased to −2 °C on DY 334. Thereafter, temperatures typically varied between −9 and −1 °C. Air temperatures only exceeded 0 °C briefly on

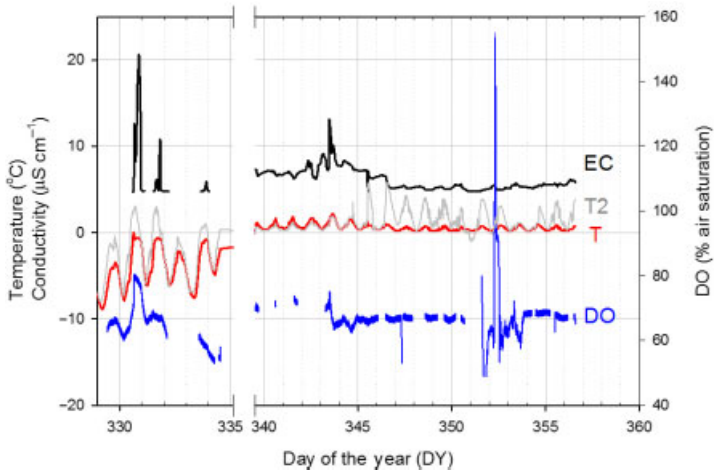

Figure 5. Time series of DO, EC, and T (dissolved oxygen, electrical conductivity, and temperature) for cryoconite hole waters at depths of 15 cm (DO, EC, and T) and 5 cm (T2) below the surface on Canada Glacier in November–December 2008

three occasions, on DY 347, 353, and 354. Air temperatures dropped markedly on DY 349 for two days, reaching −10 °C on DY 351.

Figure 5 shows the temperature of first ice (T <0 °C) and then water (T >0 °C) in the cryoconite hole, at depths of 15 cm below the ice surface and some 5 cm above the sediment layer (T), and 5 cm below the surface (T2). DO and EC values are also shown. The ice and water temperatures were always higher than the ambient air temperature (Figure 4), due to the solar heating of the cryoconite ice and basal debris layer, and the consequent incremental heating of the surrounding ice. They also varied on a daily basis, from −9 to −1 °C at the start of the sampling period. The general pattern of the ice temperatures recorded more closely follows variations in SR than air temperature, taking into account the general progressive net daily warming of the ice. Melt occurred for a few hours on DY 331, 332, and 334, and this coincided with the first recorded DO and EC values. Daily maximum water temperatures of between 0·5 and 1·8 °C were typical, although temperatures near 0 °C suggest that some freezing occurred on several of the days. It is, however, unlikely that all the water froze after DY 340 because temperatures never fell below 0 °C.

The EC records relatively high values (∼21 and ∼11 µS cm^{-1}) on the first and second days of melt, just after the peak in water temperature, as the relatively dilute first icemelt (∼5 µS cm^{-1}) refreezes as a result of the diurnal decrease in sun angle. On the third day of melting, the peak in EC is only 6 µS cm^{-1}, that of dilute glacier ice. The subsequent EC record from DY 339 onwards, when water is always present in the hole, is likely produced by a combination of inflowing water and the relative degrees of melting (which generally serves to decrease EC, because of the low solute content of glacier ice) and freezing (which increases EC) throughout the hole.

The continuity of the DO time series is compromised by brief periods of electronic failure caused by cold temperatures, particularly in the early sampling season (see Bagshaw *et al.*, 2010b for details). This was managed by the regular application of an external heat pack, but there were discontinuities in the dataset at DY 332, 340–343, and 351. However, the first DO measurements coincided with the first production of meltwater, and are values similar to those found in the P : R experiments: 50 to 80% saturation (explained below). The first DO reading was on DY 329, when the ice temperature peaks at −2 °C. This was probably the result of the DO sensor not being in exactly the same location as the thermistor, or some slight local heating of the minisensor. DO measurements were recorded continuously from DY 343 onwards, when the control module was sufficiently warm enough to function, and values of 63–72% saturation were recorded. A major DO excursion occurred on DY 352 through 354, when values as high as 152% and as low as 48% were recorded. The corresponding variation in EC throughout this period was ± 0·5 µS/cm (∼10%).

Figure 6 shows the results of the P : R experiments. The oxygen saturation of the dark incubations was relatively stable, between 60 and 76%. The saturation of

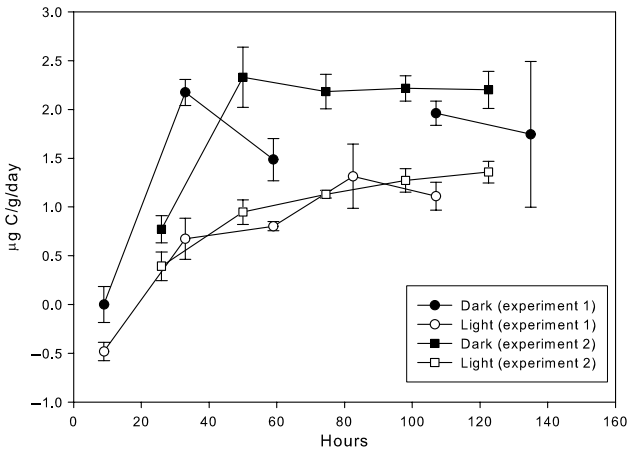

Figure 6. Photosynthesis (light) and respiration (dark) rates from two field incubations of cryoconite sediment and meltwater. Experiment 1 was in full sunlight, experiment 2 was immersed in 10 cm lake water at DLH pond. Respiration exceeds photosynthesis throughout both experiments

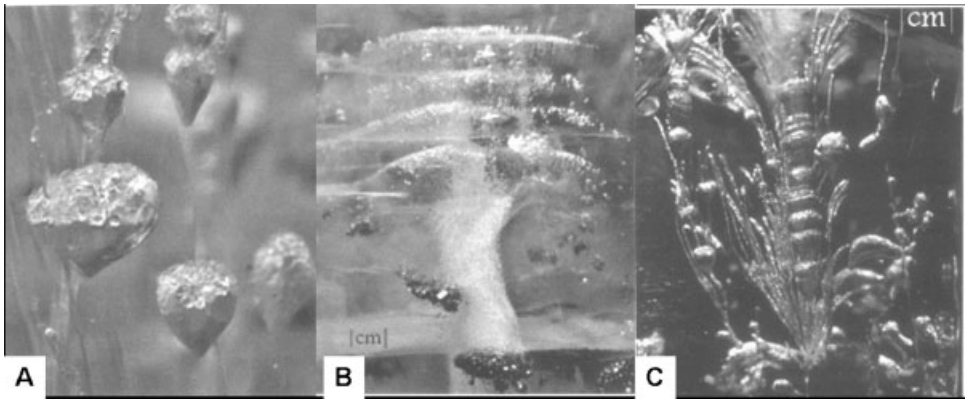

Figure 7. Bubble formation in Dry Valley lake ice covers (Adams *et al*., 1998). Bubbles form a characteristic teardrop shape, thought to also occur when cryoconite holes freeze from the sides and base

the light bottles ranged from 76 to 105%, with a mean of 91% over both experiments. P (light bottles) and R (dark bottles) increased during both experiments. R stabilized after 48 h at approximately 2·2 μg C/g/day. P continued to increase throughout both experiments, from 0·4 to 1·4 μg C/g/day, although the rate of increase slowed after approximately 40 h. R always exceeded P over the course of both incubations, and thus the incubations always exhibited net heterotrophy. These very simple representations of the cryoconite hole system show that environments with these particular rock : water ratios and PAR conditions are usually dominated by R when there are no other confounding influences.

DISCUSSION

Oxygen saturation in a closed aquatic environment is driven by a variety of physical and biogeochemical factors. Oxygen is released into solution during the melting of glacier ice, which contains bubbles of atmospheric gas. Oxygen also accumulates in solution during freezing, since gas is excluded from growing ice crystals (Adams *et al*., 1998) and during periods of net photosynthesis. Oxygen is removed from solution during periods of net respiration and oxidation of minerals containing reduced S (IV) and Fe (II) species (Tranter *et al*., 2002). The undersaturated waters in the hydrologically open cryoconite hole suggest that respiration may exceed photosynthesis, which agrees with the outcome of our short P : R incubations (Figure 6), although the absolute DO values are lower than the light incubations. Supraglacial waters at the Haut Glacier d'Arolla, Switzerland, were similarly undersaturated, ranging from 43 to 69% (Brown *et al*., 1994), and previous point measurements in cryoconite holes on Canada Glacier by Tranter *et al*., (2004) and Bagshaw (unpublished data) range from 55 to 160%.

Primary production rates in cryoconite sediment have been measured in a range of locations, often using different techniques. Rates from Svalbard vary from 0·2 μg C/g/day at Werenskioldbreen (Stibal *et al*., 2008) to 48 μg C/g/day at Austre Brøggerbreen, 208 μg C/g/day at Vestre Brøggerbreen and 353 μg C/g/day at Midre Lovenbreen, (Anesio *et al*., 2009). A value of 115 μg C/g/day was recorded at Frøya Glacier, Greenland (Anesio *et al*., 2009), and a mean of 24·4 μg C/g/day at the Vestfold Hills, Antarctica (Hodson *et al*., 2010). On the basis of these observations, some authors argue that the supraglacial environment is net autotrophic (Sawstrom *et al*., 2002; Anesio *et al*., 2009), and thus a net consumer of CO_2, whilst others argue that the system is net heterotrophic and a store of carbon (Stibal *et al*., 2008), or that there is close coupling between the two processes and, hence, the systems are predominantly in balance (Hodson *et al*., 2010). The DO time series (Figure 5) shows that net heterotrophy is found in the hydrologically connected cryoconite holes of Canada Glacier, as do our incubation results, perhaps because our P measurements (1·3 μg C/g/day) are at the lower end of the C uptake rates recorded on glaciers to date. However, previous point measurements of pH on Canada Glacier (Tranter *et al*., 2004, and Tranter and Bagshaw, unpublished data) have suggested that net P may occur, with pH values of up to 11 recorded in closed cryoconite holes. We therefore suggest that both states are possible, and that the balance between them may be controlled by local physical and biogeochemical conditions.

The first daily melt-freeze cycle occurs on DY 330 (Figure 5), when water temperatures reached 0 °C. EC values increase during melting and become even higher during the initial stages of freezing, before returning to lower values. Similar patterns are seen on two of the next three days (DY 331 and 333), but the highest EC values decline on successive days. A number of confounding factors may give rise to this patterning. The first ice melt is likely around the probe and wire connected to the logger box, which will absorb slightly more radiation than the surrounding ice. The deionized water which was used to freeze the probes into place during installation may melt, causing a small accumulation of dilute water around the EC wire and probe. In addition, the pattern of declining EC during the first days of freezing suggests that solute is moved from the vicinity of the probes by melt-freeze cycles, or that the solute in the holes is diluted by fresh glacier ice melt. The holes initially melt internally at the sediment layer, initially situated

approximately 5 cm below the probes. Glacier ice below the sediment also melts, as a result of thermal conduction through the sediment, and it is by this process that the holes melt deeper into the glacier (Podgorny and Grenfell 1996). When solar radiation input decreases at the end of each day in the early season, due to mountain shading, the hole partially refreezes. Freezing proceeds from the base and walls of the hole because of conductive heat loss to the cold glacier ice. Solutes and gases rejected from the freezing lattice are thus transported upwards through the hole and eventually freeze near the base of the overlying ice lid. The bubble pattern produced by this type of freezing is shown very elegantly within cryoconite holes in the nearby lake ice (Adams *et al*., 1998), an example of which is shown in Figure 7. Consequentially, the solute concentration of the initial meltwater in the vicinity of the EC probe decreases over time, as solutes from the concentrated early melt fraction are displaced by dilute waters from the melting glacier ice below. The first DO values also decrease in successive days (Figure 5), likely for the same reason.

The continuous EC record in Figure 5 from DY 339 onwards shows a rise to high values on DY 343, followed by a decrease between DY 343 and 347. The DO time series is not continuous during this EC excursion, but the available data suggest that there is only a small excursion in DO at best. The rise to maximum values of EC occurs when both air and water temperatures are increasing (Figure 5), so local freezing cannot be the cause of the increase. We interpret this high EC-intermediate DO signal as evidence that the hole is part of a connected system, where concentrated waters from other upstream environments which have forged a hydrological connection with the monitored hole transit through the hydrological system. This may include solute-rich cryoconite holes which were formerly disconnected from the drainage system (Bagshaw *et al*., 2007) or other waters which have been freeze-concentrated. The activity and connectivity of the subsurface drainage system is likely to vary temporally, given the propensity of the connections to melt and freeze. This is illustrated on DY 345, where the upper temperature probe (T2, Figure 5) begins to record higher-frequency temperature fluctuations. This suggests that the hole partially drained and thus the upper probe was stranded in the air head space. A small variation in EC is simultaneously detected. This stochastic drainage behaviour is also exhibited by the larger-scale cryolakes on Canada Glacier (Bagshaw *et al*., 2010a).

The water in the cryoconite hole exhibited the opposite behaviour from DY 352 onwards, when DO varied widely but there was relatively little change in EC. Cloudy conditions for four days prior to the event resulted in a reduction of solar radiation, and consequently, in air and water temperatures (to $-10\,^{\circ}$C in Figure 4, and T2 $<0\,^{\circ}$C, Figure 5). Some of the water in the vicinity of the probes likely froze, producing conditions similar to the very early season. The large perturbations in DO, however, may be caused by a variety of factors. The first could be formation of ice crystals on the sensor tip. The melting of the sediment layer into the glacier ice could also liberate more DO in the vicinity of the probe. In addition, the passage of highly oxygenated or depleted waters through the hole could influence the concentration at the sensor tip, although this is unlikely in very cold conditions when connecting passageways are frozen. Another explanation could be the result of complex interactions between freezing and drainage processes. Freezing of the holes in general leads to disconnection from the local drainage system, which causes the holes to act as closed systems. Subsequent progressive freezing of the disconnected holes then will drive DO values towards supersaturation. However, since there is no associated rise in EC and the hydrological setting of the hole suggests that it is at least sporadically connected, this scenario is unlikely in our monitored cryoconite hole.

Values of DO could decrease during internal melting of the holes which causes the air head space (Figure 1) to expand. The partition of oxygen between water and air is determined by the Henry's Law constant ($10^{-2.66}$ M/atms at $0\,^{\circ}$C), which is the ratio of the dissolved oxygen concentration to the gaseous oxygen concentration. Oxygen and other gases thus preferentially reside in the head space rather than in solution. Further expansion of the head space results in diffusion of oxygen from solution into the head space (Figure 1). Freezing processes, therefore, result in the redistribution of oxygen between the liquid and gaseous phases in the cryoconite hole. The precise values of oxygen supersaturation and undersaturation in a closed system depend on factors such as the initial DO and the ratio of water to air in the cryoconite hole. Additionally, biological factors such as the balance between respiration and photosynthesis of microorganisms in the basal sediment during melting and freezing impacts on the DO values obtained. However, the high DO observed on DY 352 may be in part caused by 'freeze-squeezing' of oxygen and other gases into solution. Evidence for the occurrence of these processes can be observed when piercing the lids of closed cryoconite holes, when water may jet out up to 1–2 m high (Fountain *et al*., 2004) as a result of the build-up of air pressure in the head space. It is likely that this pressure increase is one of the driving forces behind the forging of hydrological connections between cryoconite holes and other components of the near-surface drainage system.

We illustrate the potential of freezing around the edge of hole and the ice lid to squeeze the gas head space, and hence increase DO, as follows. The size of the head space of the hole was not measured, but previous measurements in similar holes show that the head space ranges from 0 to 7 cm, with a mean of 3 cm (Bagshaw *et al*., 2007). We assume that the headspace is 40 cm in diameter, and approximately 3 cm deep. The total depth of the hole is assumed to be 20 cm, consistent with the original placement of the sensors and measurements of water depths in similar cryoconite holes on Canada Glacier (Fountain *et al*., 2004; Bagshaw *et al*., 2007). Let us assume that the ice lid is 3 cm thick, and that the water depth is therefore 14 cm. The volume of water in the hole

is hence of the order of 18·6 l, and that of air is 3·77 l. If we assume that 5 cm of water freezes at the sides and top of the hole, and that the bottom of the hole does not freeze because of thermal inertia in the cryoconite debris, then 5·80 l of liquid remains. The new ice has density 0·915 g/cm^3 at 0 °C, compared with that of water at 0·999 g/cm^3 at 0 °C. The new ice hence occupies a larger volume than the original water, and so the head space contracts from 3·77 to 2·69 l. This decreases the head space by ∼40%. Mass balance of O_2 within the hole and the requirements of the Henry's Law constant for partition of oxygen between the dissolved and gas phases increases the DO by 56%. The volume of water has decreased by a factor of ∼3, and one would therefore anticipate that the EC would likewise increase by a similar order of magnitude. However, the EC of these dilute waters is more a consequence of pH rather than total dissolved solids, and the pH is set by the dissolution and dissociation of CO_2 into solution. Simple calculations suggest that EC will rise by a factor of ∼70%. It will be much less if the dissolved CO_2, otherwise known as carbonic acid, dissolves any mineral particulates because the specific conductance of the major cations liberated is much lower than that of H^+ ions.

Rapid changes in oxygen saturation in cryoconite holes may therefore be controlled by both physical and biological processes. Freeze-thaw cycles within the holes are precipitated by changes in air temperature, which in turn may affect the oxygen saturation. The ice lid of the holes and the thermal inertia of the solar heated sediment layer insulates them from extreme variations in temperature (Fountain *et al*., 2004; Fountain *et al*., 2008), with water temperatures being consistently above zero, but nevertheless they are affected by daily and seasonal fluctuations in solar radiation. It has been suggested that cryoconite holes act similarly on a broad scale, but that local variations in ice properties, solute concentrations, biological activity, and the degree of hydrological connection will control specific biogeochemical behaviour (Fountain *et al*., 2008). The processes occurring in this single cryoconite hole are likely similar to those occurring in other cryoconite holes on the glacier surface, but the specific timing will be controlled by individual hole properties. The varying size of the holes will govern the individual freeze-thaw dynamics, and hence, the actual DO concentration. A network of sensors in multiple holes with varying hydrological properties would be required to determine how these fluctuations operate on a glacier-wide scale, and hence to understand the processes which govern the biogeochemical effects of freeze-thaw in supraglacial drainage structures. Nevertheless, our short dataset suggests that simple relationships between DO and biogeochemical processes are more complex than we anticipated, since there are likely to be confounding physical effects of melting, freezing, and hydrological connectivity.

CONCLUSIONS

This study has presented the first high-resolution DO time series from an ice-lidded cryoconite hole on a cold-based glacier in the McMurdo Dry Valleys of Antarctica. A fibre optic DO minisensor was installed in a hydrologically connected cryoconite hole, which melted out internally and connected to the subsurface drainage system. DO ranged from 50 to 155%, values that fall within the range of past point measurements in similar holes. The water in the hole remained close to the mean of 66% throughout most of the measurement period, suggesting that the drainage system is one in which there is net respiration. Simple incubation experiments using cryoconite sediment and glacial meltwater showed that simple analogous model systems are usually dominated by respiration, with DO values similar to those observed in the hole.

The combination of EC, T, and DO measurements can be used to document the first melting and subsequent connection of the cryoconite hole to the surrounding subsurface drainage system. Partial drainage of the hole is recorded, suggesting that periodically elements of the subsurface drainage system become blocked or that flow is diverted elsewhere. The passage of waters from a variety of upstream sources is recorded via changes in EC that may or may not be associated with variations in DO. Disconnection of the cryoconite hole from the surrounding drainage system as a result of freezing, for example, as a consequence of very low air temperatures, may drive up the DO content of the water, and subsequent internal re-melting of the holes may drive down the DO as oxygen diffuses into the expanding air head space. Hence, it is likely that melt-freeze cycles result in highly variable DO.

Fibre optic sensors are a novel method for monitoring oxygen in glacial aquatic environments, capable of generating high-resolution, *in situ* data. The application of such technologies to the glacial environment will present challenges, such as those shown here, and discussed in detail in Bagshaw *et al*. (2010b), but they represent an excellent alternative to traditional sampling methods when used in conjunction with physical data and controlled biological monitoring. The development of high-resolution, automated sensors, such as those presented here, gives us an excellent opportunity to increase our understanding of aquatic biological processes in extremely cold polar glacial environments.

ACKNOWLEDGEMENTS

This work was supported by EPSRC Grant EP/D057620 /1, and NSF Grant ANT-0423595. Fieldwork was conducted with the MCMDV LTER site team whose support is gratefully acknowledged, with logistics provided by Raytheon Polar Services and PHI Helicopters. Owain Bayley assisted in the manufacture and setting up of thermistors, and Hassan Basagic was of great assistance in the field. The manuscript was greatly improved by the comments of three anonymous reviewers.

REFERENCES

Adams EE, Priscu JC, Fritsen CH, Smith SR, Brackman SL. 1998. *Permanent Ice Covers of the McMurdo Dry Valley Lakes, Antarctica: Bubble Formation and Metamorphism*. Ecosystem Processes in a Polar Desert: The McMurdo Dry Valleys, Antarctica. **72**: 281–295.

Anesio AM, Hodson AJ, Fritz A, Psenner R, Sattler B. 2009. High microbial activity on glaciers: importance to the global carbon cycle. *Global Change Biology* **15**(4): 955–960. DOI:10.1111/j.1365–2486.2008.01758.x.

Bagshaw EA, Tranter M, Fountain AG, Basagic H, Wadham JL. 2010a. Dyanmic behaviour of supraglacial lakes on cold, polar glaciers: Canada Glacier, McMurdo Dry Valleys, Antarctica. *Journal of Glaciology* **56**(196): 366–368.

Bagshaw EA, Tranter M, Fountain AG, Welch KA, Basagic H, Lyons WB. 2007. Biogeochemical evolution of cryoconite holes on Canada Glacier, Taylor Valley, Antarctica. *Journal of Geophysical Research-Biogeosciences* **112**(G4): 8. DOI:G04S35 10.1029/2007jg000442.

Bagshaw EA, Wadham JL, Mowlem M, Eveness J, Fountain AG, Tranter M, Telling J. 2010b. Determination of dissolved oxygen in the cryosphere: a comprehensive laboratory and field evaluation of fibre optic sensors. *Environmental Science and Technology.* DOI:10.1021/es102571j.

Brown GH, Tranter M, Sharp MJ, Davies TD, Tsiouris S. 1994. Dissolved oxygen variations in Alpine glacial meltwaters. *Earth Surface Processes and Landforms* **19**(3): 247–253.

Bryan JR, Riley JP, Williams PJL. 1976. Winkler procedure for making precise measurements of oxygen concentration for productivity and related studies. *Journal of Experimental Marine Biology and Ecology* **21**(3): 191–197.

Carpenter JH. 1965. The Chesapeake Bay Institute technique for the Winkler Dissolved Oxygen method. *Limnology and Oceanography* **10**(1): 141–143.

Clark LC, Wolf R, Granger D, Taylor Z. 1953. Continuous recording of blood oxygen tensions by polarography. *Journal of Applied Physiology* **6**(3): 189–193.

Cowan DA, Tow LA. 2004. Endangered Antarctic environments. *Annual Review of Microbiology* **58**: 649–690.

Doran PT, McKay CP, Clow GD, Dana GL, Fountain AG, Nylen T, Lyons WB. 2002. Valley floor climate observations from the McMurdo dry valleys, Antarctica, 1986–2000. *Journal of Geophysical Research-Atmospheres* **107**(D24): 4772. DOI: 10.1029/2001JD002045.

Doran PT, McKay CP, Fountain AG, Nylen T, McKnight DM, Jaros C, Barrett JE. 2008. Hydrologic response to extreme warm and cold summers in the McMurdo Dry Valleys, East Antarctica. *Antarctic Science* **20**(5): 499–509. DOI:10.1017/s0954102008001272.

Esposito RMM, Horn SL, McKnight DM, Cox MJ, Grant MC, Spaulding SA, Doran PT, Cozzetto KD. 2006. Antarctic climate cooling and response of diatoms in glacial meltwater streams. *Geophysical Research Letters* **33**(7): 4. DOI:L07406 10.1029/2006gl025903.

Foreman CM, Sattler B, Mickuki J, Porazinska DL, Priscu JC. 2007. Metabolic Activity of Cryoconites in the Taylor Valley, Antarctica. *Journal of Geophysical Research: Biogeosciences* **112**(G4): G04S32.

Foreman CM, Wolf CF, Priscu JC. 2004. Impact of episodic warming events on the physical, chemical and biological relationships of lakes in the McMurdo Dry Valleys, Antarctica. *Aquatic Geochemistry* **10**(3): 239–268.

Fortner SK, Tranter M, Fountain A, Lyons WB, Welch KA. 2005. The geochemistry of supraglacial streams of Canada Glacier, Taylor Valley (Antarctica), and their evolution into proglacial waters. *Aquatic Geochemistry* **11**(4): 391–412.

Fountain AG, Lyons WB, Burkins MB, Dana GL, Doran PT, Lewis KJ, McKnight DM, Moorhead DL, Parsons AN, Priscu JC, Wall DH, Wharton RA, Virginia RA. 1999. Physical controls on the Taylor Valley ecosystem, Antarctica. *Bioscience* **49**(12): 961–971.

Fountain AG, Nylen T, Tranter M, Bagshaw EA. 2008. Temporal variation of cryoconite holes on Canada Glacier, McMurdo Dry Valleys, Antarctica. *Journal of Geophysical Research* **112**(G01S92): DOI:10.1029/2007JG000430.

Fountain AG, Tranter M, Nylen TH, Lewis KJ, Mueller DR. 2004. Evolution of cryoconite holes and their contribution to meltwater runoff from glaciers in the McMurdo Dry Valleys, Antarctica. *Journal of Glaciology* **50**(168): 35–45.

Hodson A, Anesio AM, Tranter M, Fountain A, Osborn M, Priscu J, Laybourn-Parry J, Sattler B. 2008. Glacial ecosystems. *Ecological Monographs* **78**(1): 41–67.

Hodson A, Cameron K, Boggild C, Irvine-Fynn T, Langford H, Pearce D, Banwart S. 2010. The structure, biological activity and biogeochemistry of cryoconite aggregates upon an Arctic valley glacier: Longyearbreen, Svalbard. *Journal of Glaciology* **56**(196): 349–362.

Hoffman MJ, Fountain AG, Liston GE. 2008. Surface energy balance and melt thresholds over 11 years at Taylor Glacier, Antarctica. *Journal of Geophysical Research-Earth Surface* **113**(F4): 12. DOI:10.1029/2008jf001029.

Kennedy AD. 1993. Water as a Limiting Factor in the Antarctic Terrestrial Environment—a Biogeographical Synthesis. *Arctic and Alpine Research* **25**(4): 308–315.

Klimant I, Meyer V, Kuhl M. 1995. Fibreoptic oxygen microsensors: a new tool in aquatic biology. *Limnology and Oceanography* **40**(6): 1159–1165.

Lewis KJ, Fountain AG, Dana GL. 1999. How important is terminus cliff melt?: a study of the Canada Glacier terminus, Taylor Valley, Antarctica. *Global and Planetary Change* **22**(1): 105–115.

Lippitsch ME, Pusterhofer J, Leiner MJP, Wolfbeis OS. 1988. Fibre-optic oxygen sensor with the fluorescence decay as the information carrier. *Analytica Chimica Acta* **205**(1): 1–6.

Morgan-Kiss RM, Priscu JC, Pocock T, Gudynaite-Savitch L, Huner NPA. 2006. Adaptation and acclimation of photosynthetic microorganisms to permanently cold environments. *Microbiology and Molecular Biology Reviews* **70**(1): 222. DOI:10.1128/mmbr.70.1.222–252.2006.

Ødegärd RS, Hagen JO, Hamran SE. 1997. Comparison of radio-echo sounding (30–1000 MHz) and high-resolution borehole-temperature measurements at Finsterwalderbreen, southern Spitsbergen, Svalbard. *Annals of Glaciology* **24**: 262–267.

Podgorny IA, Grenfell TC. 1996. Absorption of solar energy in a cryoconite hole. *Geophysical Research Letters* **23**(18): 2465–2468.

Porazinska DL, Fountain AG, Nylen TH, Tranter M, Virginia RA, Wall DH. 2004. The Biodiversity and biogeochemistry of cryoconite holes from McMurdo Dry Valley glaciers, Antarctica. *Arctic Antarctic and Alpine Research* **36**(1): 84–91.

PreSens 2006. Instruction Manual Fibox 3. Regensburg.

Rogers KR, Poziomek EJ. 1996. Fiber optic sensors for environmental monitoring. *Chemosphere* **33**(6): 1151–1174.

Sawstrom C, Mumford P, Marshall W, Hodson A, Laybourn-Parry J. 2002. The microbial communities and primary productivity of cryoconite holes in an Arctic glacier (Svalbard 79 degrees N). *Polar Biology* **25**(8): 591–596.

Stibal M, Sabacka M, Kastovska K. 2006. Microbial communities on glacier surfaces in Svalbard: Impact of physical and chemical properties on abundance and structure of cyanobacteria and algae. *Microbial Ecology* **52**(4): 644–654.

Stibal M, Tranter M, Benning LG, Rehak J. 2008. Microbial primary production on an Arctic glacier is insignificant in comparison with allochthonous organic carbon input. *Environmental Microbiology* **10**(8): 2172–2178. DOI:10.1111/j.1462–2920.2008.01620.

Telling J, Anesio AM, Hawkings J, Tranter M, Wadham J, Hodson A, Irvine-Fynn T, Yallop ML. 2010. Measuring rates of gross photosynthesis and net community production in cryoconite holes: a comparison of field methods. *Annals of Glaciology* **51**(56): (in press).

Tranter M, Bagshaw EA, Fountain AG, Foreman CM. 2010. *The biogeochemistry and hydrology of McMurdo Dry Valley glaciers: is there life on Martian ice now? Life in Antarctic deserts and other cold, dry environments: Astrobiological analogues*. Doran PT, Lyons WB, McKnight DM (eds). Cambridge University Press: Cambridge, UK; 195–221.

Tranter M, Fountain AG, Fritsen CH, Lyons WB, Priscu JC, Statham PJ, Welch KA. 2004. Extreme hydrochemical conditions in natural microcosms entombed within Antarctic ice. *Hydrological Processes* **18**(2): 379–387.

Tranter M, Sharp MJ, Lamb HR, Brown GH, Hubbard BP, Willis IC. 2002. Geochemical weathering at the bed of Haut Glacier d'Arolla, Switzerland—a new model. *Hydrological Processes* **16**(5): 959–993.

Wall DH. 2007. Global change tipping points: above- and below-ground biotic interactions in a low diversity ecosystem. *Philosophical Transactions of the Royal Society B-Biological Sciences* **362**(1488): 2291–2306. DOI:10.1098/rstb.2006.1950.

Wolfbeis OS. 2008. Fiber-optic chemical sensors and biosensors. *Analytical Chemistry* **80**(12): 4269–4283. DOI:10.1021/ac800473b.

